Perfectly matched multiscale simulations for discrete lattice systems: Extension to multiple dimensions

Shaofan Li,* Xiaohu Liu, Ashutosh Agrawal, and Albert C. To
Department of Civil and Environmental Engineering, University of California, Berkeley, California 94720, USA
(Received 19 February 2006; revised manuscript received 3 May 2006; published 18 July 2006)

Extending the technique of the perfectly matched layer (PML) to discrete lattice systems, a multiscale method was proposed by To and Li [Phys. Rev. B **72**, 035414 (2005)], which was termed the perfectly matched multiscale simulation (PMMS). In this paper, we shall revise the proposed PMMS formulation, and extend it to multiple dimensions. It is shown in numerical simulations that the perfectly matched layer between the fine scale region and the coarse scale region can provide an efficient remedy to reduce spurious phonon reflections. We have found (i) the bridging projection operator stems from minimization of the temperature of an equilibrium system; (ii) for discrete lattice systems, the perfectly matched layer (PML) can be constructed by stretching the lattice constant, or the equilibrium atomic spacing, in the Fourier domain; (iii) the dispersive relation in the PML zone is significantly different from the one in the original lattice system, and the PML usually behaves like a low-frequency pass filter. This may be one of the mechanisms to eliminate the reflective waves at the multiscale interface. Moreover, we apply the multidimensional PMMS algorithm to simulate a screw dislocation passing through different scales.

DOI: 10.1103/PhysRevB.74.045418 PACS number(s): 46.15.−x, 02.70.Ns, 05.10.−a, 45.10.−b

I. INTRODUCTION

To construct the suitable match condition at the discrete-continuum interface has been a challenge in concurrent multiscale simulations. The notable contributions to this subject include E and his co-workers' optimal boundary match approach,[1–3] Liu and his co-workers' bridging scale method,[4–6] and Rudd and Broughton's coarse-grained molecular dynamics (CGMD).[7,8] However, most of these approaches are either too complicated to implement or too limited to apply to general concurrent multiscale simulations.

To effectively reduce phonon reflections at multiscale interfaces, we[9] proposed a different multiscale method called the perfectly matched multiscale simulation (PMMS), which extended the perfectly matched layer (PML) technique for continuum systems to discrete systems.

The perfectly matched layer (PML) method is a numerical technique to simulate wave (electromagnetic or acoustic) propagations in an infinite domain. It has been extensively used in many fields to eliminate spurious waves due to the mismatch of impedances at the interface of different media (e.g., Refs. 10 and 11). The features that distinguish PML from other absorbing boundary techniques are (i) PML is a reflectionless medium that has no clear interface between the domain of interests and the additional matched layer; (ii) the PML technique produces a spatial decay term (in addition to time decay) with exponential rate, and hence (iii) the PML technique provides a perfectly matched layer to link the regions with different impedances.

The original PMMS formulation is a simple extension of the PML technique for continuum to discrete lattices. Even though the proposed algorithm is correct and it worked well in computations, there were mistakes in our original construction procedures, which become apparent when extending it to multiple dimensions.

We have found that the extension of PML of the continuous media to discrete lattices is not a straightforward analog, because there are fundamental differences between wave propagations in continuous media and discrete lattices. It had been shown by Deymier and Vasseur[12] that the mismatch in coupled discrete-continuous models is inherently linked to the difference in dispersion relations of different media or models.

In this paper, we revise our previous formulation, and extend it to cases of multiple dimensions. A systematic analysis of dispersive relations in the PML zone is carried out to study the efficiency of the absorbing boundary layer or impedance matched layer for discrete systems. To validate the proposed formulation, we test the proposed algorithm in simulations of multiple dimensional problems. In particular, we apply the proposed algorithm to simulate the problem of defect passing from one scale to another scale.

The paper is organized in the following way. In Sec. II we re-visit the basic formulas of PMMS, and in Sec. III, we re-derive the equations of motion in the PML region through a different approach. In Sec. IV, we shall analyze the properties of the discrete perfectly matched layer, and finally, in Sec. V, several simulation examples are presented.

II. FORMULATIONS

Consider a continuous displacement field up to subatomic scale. We assume that the total displacement field can be decomposed into a coarse scale component and a fine scale component as proposed in the bridging scale method by Wagner and Liu,[4]

$$\mathbf{u}(\mathbf{x}) = \bar{\mathbf{u}}(\mathbf{x}) + \mathbf{u}'(\mathbf{x}), \tag{1}$$

where $\mathbf{u}$ is the total displacement field, $\bar{\mathbf{u}}$ is the coarse scale displacement field, and $\mathbf{u}'$ is the fine scale displacement field.

We can use finite element (FE) interpolation to construct the coarse scale displacement field,

$$\bar{\mathbf{u}}(\mathbf{x}) = \mathbf{N}(\mathbf{x})\mathbf{d}, \tag{2}$$

where $\mathbf{N}(\mathbf{x})$ is the finite element interpolation function, and $\mathbf{d}$ is the FE nodal displacement vector.

To link the coarse scale displacement field to the atomic displacements $\mathbf{q}$, we assume that there exists a linear operator $\mathbf{P}(\mathbf{x})$ that maps the displacements of every atom $\mathbf{q}$ to the the coarse scale displacement field,

$$\bar{\mathbf{u}}(\mathbf{x}) = \mathbf{P}(\mathbf{x})\mathbf{q}. \tag{3}$$

Note that the FE nodal points can be either a subset of atomic sites or a completely different set of particles. Hence one should consider Eq. (2) as the definition of the coarse scale displacement field, and Eq. (3) as an approximated projection. Similarly, the fine scale displacement field is determined by another mapping,

$$\mathbf{u}'(\mathbf{x}) = \mathbf{Q}(\mathbf{x})\mathbf{q}. \tag{4}$$

At the atom site, i.e., at atoms' positions, we have the following expression for displacements:

$$\mathbf{q} = \mathbf{P}\mathbf{q} + \mathbf{Q}\mathbf{q} = \mathbf{N}\mathbf{d} + \mathbf{Q}\mathbf{q}. \tag{5}$$

From the first equality, one can identify $\mathbf{Q}=\mathbf{I}-\mathbf{P}$ at the atom site, and one may extend it to assume that it is valid for the entire field, i.e., $\mathbf{Q}(\mathbf{x})=\mathbf{I}-\mathbf{P}(\mathbf{x})$.

There are different ways to obtain the expressions of projection matrices, $\mathbf{P}(\mathbf{x})$ and $\mathbf{Q}(\mathbf{x})$. In Ref. 4, for example, they are obtained by minimizing the difference between $\mathbf{q}$ and $\bar{\mathbf{u}}$ at the atom site via a L_2 projection. In the original PMMS paper, we proposed to obtain $\mathbf{P}(\mathbf{x})$ and $\mathbf{Q}(\mathbf{x})$ by minimizing the difference between total scale and coarse scale Lagrangians:

$$\min_{\mathbf{d},\dot{\mathbf{d}}}[L(\mathbf{d},\dot{\mathbf{d}};\mathbf{q},\dot{\mathbf{q}}) - \bar{L}(\mathbf{d},\dot{\mathbf{d}})], \tag{6}$$

where $L(\mathbf{d},\dot{\mathbf{d}};\mathbf{q},\dot{\mathbf{q}})=K(\dot{\mathbf{d}},\dot{\mathbf{q}})-U(\mathbf{d},\mathbf{q})$ and $\bar{L}(\mathbf{d},\dot{\mathbf{d}})=\bar{K}(\dot{\mathbf{d}})-U(\mathbf{d})$, in which K and $\bar{K}$ are kinetic energies of the fine scale and coarse scale, respectively; $U(\mathbf{d},\mathbf{q})$ and $U(\mathbf{d})$ are the fine scale and coarse scale potential energies. Note that $\dot{\mathbf{d}}$ and $\dot{\mathbf{q}}$ are velocity vectors for all particles (atoms or FE nodes) in both fine scale and coarse scale fields.This proposal turns out to be *incorrect*, because the objective function or the difference between the Lagrangians may not have a minimum. Hence instead of a minimization process, $\mathbf{P}(\mathbf{x})$ and $\mathbf{Q}(\mathbf{x})$ obtained in this way are actually at the saddle point of the objective function. To correct this error, we are now seeking the projection operators by minimizing the difference between total and coarse scale *kinetic energies*, i.e.,

$$\min_{\dot{\mathbf{d}}}[K(\dot{\mathbf{d}},\dot{\mathbf{q}}) - \bar{K}(\dot{\mathbf{d}})]. \tag{7}$$

The expressions for kinetic energies are

$$K(\dot{\mathbf{q}},\dot{\mathbf{d}}) = \frac{1}{2}(\mathbf{N}\dot{\mathbf{d}} + \mathbf{Q}\dot{\mathbf{q}})^T\mathbf{M}_A(\mathbf{N}\dot{\mathbf{d}} + \mathbf{Q}\dot{\mathbf{q}}), \tag{8}$$

$$\bar{K}(\dot{\mathbf{d}}) = \frac{1}{2}\dot{\mathbf{d}}^T\mathbf{M}\dot{\mathbf{d}}, \tag{9}$$

where $\mathbf{M}_A$ is the constant diagonal molecular-dynamics mass matrix and $\mathbf{M}(\mathbf{x})=\mathbf{N}^T(\mathbf{x})\mathbf{M}_A\mathbf{N}(\mathbf{x})$ is the finite element mass matrix.

According to Wagner and Liu,[4] the average kinetic energy may be written as

$$\begin{aligned}\langle K(\dot{\mathbf{d}},\dot{\mathbf{q}})\rangle = &\left\{\int_{\infty}^{\infty}\left(\frac{1}{2}\dot{\mathbf{d}}^T\mathbf{M}\dot{\mathbf{d}} + \frac{1}{2}\dot{\mathbf{q}}\mathcal{M}^T\dot{\mathbf{q}}\right)\right.\\ &\left.\times\exp\left[-\frac{1}{2}\beta\dot{\mathbf{q}}\mathcal{M}^T\dot{\mathbf{q}}\right]d\dot{\mathbf{q}}\right\}\\ &\times\left\{\int_{\infty}^{\infty}\exp\left[-\frac{1}{2}\beta\dot{\mathbf{q}}\mathcal{M}^T\dot{\mathbf{q}}\right]d\dot{\mathbf{q}}\right\}^{-1} = \frac{1}{2}\dot{\mathbf{d}}^T\mathbf{M}\dot{\mathbf{d}}\\ &+\frac{3}{2}k_BT(n_a - n_c),\end{aligned} \tag{10}$$

where n_a is the total number of atoms (degrees of freedom of $\mathbf{q}$) and n_c is the total number of FE nodes (degrees of freedom of $\mathbf{d}$); $\mathcal{M} := = \mathbf{Q}^T\mathbf{M}\mathbf{Q}$, and $\beta=(k_BT)^{-1}$, k_B being the Boltzmann's constant and T the temperature of the system.

Therefore, intuitively, we may link the difference in kinetic energies with the temperature of a system under equilibrium state,

$$K(\dot{\mathbf{d}},\dot{\mathbf{q}}) - \bar{K}(\dot{\mathbf{d}}) \sim T. \tag{11}$$

Hence a physical interpretation of minimizing the difference in kinetic energies, i.e., Eg. (7), may be stated as "for an equilibrium system with fixed kinetic energy, the coarse scale projection operator is obtained from the least temperature condition for all possible coarse scale velocity fields with the fixed degree of freedom n_c."

Consequently, a standard minimization procedure yields the following normal equation:

$$\mathbf{N}^T\mathbf{M}_A\dot{\mathbf{q}} - \mathbf{M}\dot{\mathbf{d}} = 0. \tag{12}$$

Multiplying the above equation by $\mathbf{N}\mathbf{M}^{-1}$ leads to

$$\mathbf{N}\dot{\mathbf{d}} = \mathbf{N}\mathbf{M}^{-1}\mathbf{N}^T\mathbf{M}_A\dot{\mathbf{q}}. \tag{13}$$

At the atom site, the decomposition (5) gives us

$$\mathbf{N}\dot{\mathbf{d}} = (\mathbf{I} - \mathbf{Q})\dot{\mathbf{q}}. \tag{14}$$

Comparing Eqs. (13) and (14), we first obtain the expression for $\mathbf{Q}$ at atom sites and then extend to the entire field,

$$\mathbf{Q}(\mathbf{x}) = \mathbf{I} - \mathbf{N}(\mathbf{x})\mathbf{M}^{-1}(\mathbf{x})\mathbf{N}^T(\mathbf{x})\mathbf{M}_A. \tag{15}$$

It follows that

$$\mathbf{P}(\mathbf{x}) = \mathbf{N}(\mathbf{x})\mathbf{M}^{-1}(\mathbf{x})\mathbf{N}^T(\mathbf{x})\mathbf{M}_A. \tag{16}$$

Again, the result is the same as the ones proposed in the bridging scale method[6,13] as well as in the original PMMS paper.[9]

III. EQUATIONS IN THE PML REGION

In the PMMS model, the PML is designed to absorb high-frequency waves coming from the fine scale region. Since the lattice structure of the fine scale region is discrete, i.e., a collection of atoms, the construction of a perfectly matched layer should be based on the template of discrete systems rather than a discretization of a continuum system. In the original PMMS paper, the equations of motion in the PML region were derived in a fashion similar to that of continuous media. We now realize that those procedures are not appropriate for the discrete case. In this paper we re-derive the equations of motion for the discrete PML zone. The approach is still similar to the complex coordinate transformation, which was first adopted by Ref. 14. But instead of stretching continuous Cartesian coordinates, we will stretch the equilibrium distance (bond length) between two atoms.

We start with a general three-dimensional (3D) lattice of N atoms. A general 3D lattice has a periodic structure. The collection of atoms that appear periodically is called the *unit cell*. Let us assume a unit cell to contain m atoms. A lattice is defined by three basis vectors $\mathbf{a}_1$, $\mathbf{a}_2$ and $\mathbf{a}_3$. The origin of each unit cell has the following coordinate:

$$\mathbf{X}(\ell) = \ell_1\mathbf{a}_1 + \ell_2\mathbf{a}_2 + \ell_3\mathbf{a}_3, \tag{17}$$

where ℓ_i are integers. So the coordinate of the jth atom in the ℓth cell is

$$\mathbf{X}(\ell,j) = \mathbf{X}(\ell) + \mathbf{X}(j). \tag{18}$$

We can write the basis vectors $\mathbf{a}_\alpha, \alpha=1, 2, 3$ as

$$\mathbf{a}_\alpha = h_\alpha \hat{\mathbf{a}}_\alpha, \tag{19}$$

where h_α is the equilibrium distance in the α direction and $\hat{\mathbf{a}}_\alpha$ is the unit vector in that direction.

We assume for now the potential energy U of the lattice to be quadratic. In terms of the displacements, it can be written as

$$U = \frac{1}{2}\sum_{\ell,j,\alpha,\ell',j',\beta} U_{\alpha\beta}(\ell,j,\ell',j')u_\alpha(\ell,j)u_\beta(\ell',j'), \tag{20}$$

where α and β denote Cartesian components and

$$U_{\alpha\beta}(\ell,j,\ell',j') = \frac{\partial^2 U}{\partial u_\alpha(\ell,j)\partial u_\beta(\ell',j')}. \tag{21}$$

For quadratic potentials, we can write U as

$$U = \frac{1}{2}\sum_{\ell,j,\alpha,\ell',j',\beta} C_{\alpha\beta}(\ell,j,\ell',j')\frac{u_\alpha(\ell,j)}{h_\alpha}\frac{u_\beta(\ell',j')}{h_\beta}. \tag{22}$$

The new force constant $C_{\alpha\beta}(\ell,j,\ell',j')$ now has the unit of work. The equations of motion for each atom then read

$$m_i\ddot{u}_\alpha(\ell,j) = -\sum_{\ell',j',\beta}\frac{C_{\alpha\beta}(\ell,j,\ell',j')}{h_\alpha h_\beta}u_\beta(\ell',j'), \tag{23}$$

where m_i is the mass of the atom i.

We view the PML region as an outside layer of the original lattice. So it is of the same type of lattice as the original one. The interface between the original lattice and the PML region will be simply called "the interface" from now on. Now we want to derive the EOM in the PML region. Let us first consider the EOM in the frequency domain, which reads

$$-m_i\omega^2\hat{u}_\alpha(\ell,j) = -\sum_{\ell',j',\beta}\frac{C_{\alpha\beta}(\ell,j,\ell',j')}{h_\alpha h_\beta}\hat{u}_\beta(\ell',j'), \tag{24}$$

where $\hat{\mathbf{u}} := = \mathcal{F}(\mathbf{u})$ is the Fourier transform of $\mathbf{u}$ and ω is the angular frequency.

Now we stretch the equilibrium distances h_γ into a complex number

$$h_\gamma \to h_\gamma\left(1 + \frac{d_\ell}{i\omega}\right), \quad \gamma = \alpha,\beta, \tag{25}$$

where d_ℓ is a damping function depending on particle positions (the cell ℓ). And to maintain the same lattice symmetry, we only consider isotropic damping, i.e., d_ℓ is the same in all lattice directions. We shall talk more about d_ℓ later. Using the stretched h_γ in the PML region, the equation of motion in the frequency domain now reads

$$\left(1 - \frac{d_\ell^2}{\omega^2} - i\frac{2d_\ell}{\omega}\right)m_i\omega^2\hat{u}_\alpha(\ell,j) = -\sum_{\ell',j',\beta}\frac{C_{\alpha\beta}(\ell,j,\ell',j')}{h_\alpha h_\beta}\hat{u}_\beta(\ell',j'). \tag{26}$$

Taking the inverse Fourier transform, we obtain the equation of motion in the PML region:

$$m_i\ddot{u}_\alpha(\ell,j) - 2m_i d_\ell\dot{u}_\alpha(\ell,j) - m_i d_\ell^2 u_\alpha(\ell,j) = -\sum_{\ell',j',\beta}\frac{C_{\alpha\beta}(\ell,j,\ell',j')}{h_\alpha h_\beta}u_\beta(\ell',j'). \tag{27}$$

By inspection, the above equation now has a damping term $-2m_i d_\ell u_\alpha$ and a change in stiffness $-m_i d_\ell^2 u_\alpha$. It is obvious that if $d_\ell=0$ in the original lattice, we recover the equations of motion for original molecular-dynamics (MD) simulation.

Remark 1. (i) In the existing literature, the so-called lattice PML is just discretization of continuum PML via a stencil, which is simply a numerical object that has no clear physical meaning. The discrete PML proposed in this work is built on a true discrete template from the outset, and it originates from the stretching the lattice constant. To understand the physical meaning of such an operation, we define the complex stiffness

$$\hat{C}_{\alpha\beta} = \frac{C_{\alpha\beta}}{\left(1 + \frac{d_\ell}{i\omega}\right)^2}. \tag{28}$$

Thus Eq. (26) may read

$$m_i\omega^2\hat{u}_\alpha(\ell,j) = -\sum_{\ell',j',\beta}\frac{\hat{C}_{\alpha,\beta}(\ell,j,\ell',j')}{h_\alpha h_\beta}\hat{u}_\beta(\ell',j') \tag{29}$$

which means that the physical meaning of stretching the equilibrium bond distance may be interpreted as or accomplished by insertion of the complex stiffness coefficients for atomic bonds. In other words, the PML for MD may be

characterized as an absorbing boundary layer with complex material constants within the PML layer. This indicates that the PML layer for MD is a lossy medium.

(ii) For a general nonlinear potential U, we may first use its harmonic approximation in the PML region, i.e.,

$$U \approx U^{harmonic} = U(h_1,h_2,h_3) + \frac{1}{2}\sum_{\ell,j,\alpha,\ell',j',\beta} U_{\alpha\beta}(\ell,j,\ell',j')u_\alpha(\ell,j)u_\beta(\ell',j'). \tag{30}$$

However, the above equilibrium atom spacing stretching technique may be applied to anharmonic potentials as well. We shall discuss two examples. To make the expressions simpler, we assume that the lattice constants are the same in all three directions, i.e.,

$$h_1 = h_2 = h_3 = h \tag{31}$$

(iii) In the first example, we consider the homogeneous anharmonic potential function of Nth order ($N \neq 2$),

$$U(r) = \sum_{n,m} \phi\left(\frac{r_{mn}}{h}\right), \quad \text{where } \phi(\alpha r) = \alpha^n \phi(r),$$

where $\phi(r)$ is the atomistic potential, and m denotes all atoms interacting with atom n. The equation of motion then reads

$$m_n \ddot{\mathbf{u}}_n = \mathbf{f}_n = -\frac{\partial U(r)}{\partial \mathbf{u}_n} = -\sum_m \phi'(r_{mn})\frac{\mathbf{u}_n - \mathbf{u}_m}{h^N r_{mn}}. \tag{32}$$

In the Fourier domain, we have the following equation:

$$m_n\omega^2 \hat{\mathbf{u}}_n = \sum_m \frac{1}{h^N}\mathcal{F}\left\{\phi'(r_{mn})\frac{\mathbf{u}_n - \mathbf{u}_m}{r_{mn}}\right\}. \tag{33}$$

Choosing the following atomic distance stretching scheme:

$$h \to h\left(1 + \frac{d(\mathbf{X}_n)}{i\omega}\right)^{1/N}, \tag{34}$$

where $d(\mathbf{X}_n)$ is a damping function of the initial position of atom n, we then obtain

$$m_n\omega^2\left(1 + \frac{d(\mathbf{X}_n)}{i\omega}\right)\hat{\mathbf{u}}_n = \sum_m \frac{1}{h^N}\mathcal{F}\left\{\phi'(r_{mn})\frac{\mathbf{u}_n - \mathbf{u}_m}{r_{mn}}\right\} \tag{35}$$

and the inverse Fourier transform gives the following equation of motion for the PML zone:

$$m_n\ddot{\mathbf{u}}_n + m_n d(\mathbf{X}_n)\dot{\mathbf{u}} = -\sum_m \frac{1}{h^N}\phi'(r_{mn})\frac{\mathbf{u}_n - \mathbf{u}_m}{r_{mn}}. \tag{36}$$

Or we can choose another atomic distance stretching scheme,

$$h \to h\left(1 + \frac{d(\mathbf{X}_n)}{i\omega}\right)^{2/N}, \tag{37}$$

which leads to the following equations:

$$m_n\omega^2\left(1 + \frac{d(\mathbf{X}_n)}{i\omega}\right)^2\hat{\mathbf{u}}_n = \sum_m \frac{1}{h^N}\mathcal{F}\left\{\phi'(r_{mn})\frac{\mathbf{u}_n - \mathbf{u}_m}{r_{mn}}\right\} \tag{38}$$

in the Fourier domain. Subsequently, the inverse Fourier transform gives the following equations of motion for PML zone:

$$m_n\ddot{\mathbf{u}}_n - 2m_n d(\mathbf{X}_n)\dot{\mathbf{u}} - m_n d^2(\mathbf{X}_n)\mathbf{u} = -\sum_m \frac{1}{h^N}\phi'(r_{mn})\frac{\mathbf{u}_n - \mathbf{u}_m}{r_{mn}} \tag{39}$$

In the second example, we consider the Lennard-Jones potential,

$$\phi(r_{mn}) = 4\epsilon\left[\left(\frac{\sigma}{r_{mn}}\right)^{12} - \left(\frac{\sigma}{r_{mn}}\right)^6\right], \quad \text{with } h = 2^{1/6}\sigma \tag{40}$$

and

$$\frac{\partial\phi}{\partial\mathbf{u}_n} = 24\epsilon\left[-2\left(\frac{\sigma}{r_{mn}}\right)^{12} + \left(\frac{\sigma}{r_{mn}}\right)^6\right]\frac{\mathbf{u}_n - \mathbf{u}_m}{r_{mn}^2} = \phi'(r_{mn})\frac{\mathbf{u}_n - \mathbf{u}_m}{r_{mn}}. \tag{41}$$

Choose the following stretching scheme:

$$h \to h\left(1 + \frac{d(\mathbf{X}_n)}{i\omega}\right)^{-1/6}. \tag{42}$$

The transformed equation of motion in the PML zone is

$$m_n\omega^2\left(1 + \frac{d(\mathbf{X}_n)}{i\omega}\right)^2\hat{\mathbf{u}}_n = \sum_m \mathcal{F}\left\{\phi'(r_{mn})\frac{\mathbf{u}_n + \mathbf{u}_m}{r_{mn}}\right\} - 24\epsilon\left(\frac{d(\mathbf{X}_n)}{i\omega}\right)\mathcal{F}\left\{\left(\frac{\sigma}{r_{mn}}\right)^6\frac{\mathbf{u}_n - \mathbf{u}_m}{r_{mn}^2}\right\}, \tag{43}$$

where $\mathcal{F}$ is the operator of Fourier transform. The equation of motion in the PML zone for the Lennard-Jones potential is obtained by taking the inverse Fourier transform:

$$m_u\ddot{\mathbf{u}}_n - 2m_n d(\mathbf{X}_n p)\dot{\mathbf{u}}_n - m_n d^2(\mathbf{X}_n)\mathbf{u}_n = -\sum_m \left\{\phi'(r_{mn})\frac{\mathbf{u}_n - \mathbf{u}_m}{r_{mn}} - 24\epsilon d(\mathbf{X}_n) \cdot \int_0^t \left(\frac{\sigma}{r_{mn}(t-\tau)}\right)^6 \frac{\mathbf{u}_n(t-\tau) - \mathbf{u}_m(t-\tau)}{r_{mn}^2(t-\tau)}d\tau\right\}. \tag{44}$$

In the rest of this paper, without loss of generality, we shall focus on the case of harmonic approximation.

IV. ANALYSIS OF DISCRETE PML

We now study the behaviors of lattice PML and its related PMMS method. Since the primary function of the PML zone is to serve as an absorbing boundary, we want the solution in the PML zone to have two properties: (i) *spatial decay*, i.e., the wave solution should attenuate when exiting the interface toward the PML region; (ii) *perfectly matched*, i.e., the im-

pedance at the multiscale interface should be matched. Both properties hold true for conventional PML of continuous media with an appropriate choice of damping function $d(\mathbf{X})$. In actual computations, if FE or finite difference (FD) are used in discretization of a continuum, there will be reflections at the interface. To estimate the reflection, a reflection coefficient, which is the amount of displacement being reflected back at the interface, is often computed. In the following, we want to answer two questions: (i) Do the two properties hold true for the lattice PML? (ii) If there is reflection at interface, what is the value of the reflection coefficient?

Furthermore, it is well known that in continuous media traveling waves can have arbitrary frequencies in principle. Whereas in a discrete lattice, only waves with certain frequencies can propagate. This property is called *dispersion*.[15,16] Dispersion is a fundamental nature of lattice dynamics, and it has been studied extensively in the past.[15–18] In this section, we focus on studying dispersion relations in the PML region and its effects on eliminating spurious phonon reflections.

A. Wave solution in PML zone

We first consider the following general traveling-wave solution:

$$u_\alpha(\ell,j) = A_\alpha(j)e^{i[\omega t - 2\pi \mathbf{k}\cdot\mathbf{X}(\ell)]}, \tag{45}$$

where $\mathbf{k}$ is the wave vector.

We then stretch the equilibrium distance in every crystallographic direction:

$$h_\alpha \to h_\alpha\left(1 + \frac{d_\ell}{i\omega_0}\right). \tag{46}$$

Here ω_0 denotes as a fixed frequency. Since both d_ℓ and ω_0 are our choices, for the sake of simplicity, we can combine them together into a new damping function $d(\ell,\omega_0)$:

$$d(\ell,\omega_0) = \frac{d_\ell}{\omega_0}. \tag{47}$$

We will adopt this notation from here on. The basis vectors will be stretched as

$$\mathbf{a}_n \to \mathbf{a}_n(1 - id). \tag{48}$$

The position vector $\mathbf{X}(\ell)$ will be stretched as

$$\mathbf{X}(\ell) \to \mathbf{X}(\ell)(1 - id). \tag{49}$$

Substitute the above relationship back into Eq. (45); we obtain the stretched solution, i.e., the solution in the PML region:

$$u_\alpha(\ell,j) = A_\alpha(j)e^{i[\omega t - 2\pi \mathbf{k}\cdot\mathbf{X}(\ell)]}e^{-2\pi d\mathbf{k}\cdot\mathbf{X}(\ell)}. \tag{50}$$

Immediately, we find that the PML solution has a spatial decaying term $e^{-2\pi d\mathbf{k}\cdot\mathbf{X}(\ell)}$ that is the hallmark of the PML for continuous media. So we will have the desired property as long as Eq. (50) is indeed the solution of Eq. (27).

Remark 2. (i) The derivation given in Ref. 9 essentially relies on Eq. (49). Therefore if the harmonic approximation is adopted, all the results in Ref. 9 will hold. (ii) In the solution (50), the frequency depends on the wave number. This brings out the issue of dispersion. (iii) Usually, the original lattice possesses certain symmetry or anisotropy, e.g., a hexagonal lattice, or a cubic lattice, etc. The corresponding PML zone should have the same symmetry or anisotropy as that of the original lattice. This means that the stretched lattice structure in the PML zone should maintain the same symmetry in accordance with that of the original lattice system, such that they can be perfectly matched, whereas in construction of a continuous PML, the distinctive coordinate stretching may be performed along the three directions of the Cartesian coordinates. This is another major difference between discrete PML and continuous PML.

B. Dispersion in the PML zone

For a self-contained presentation, we first review the concept of dispersion in a simple lattice. Consider a one dimensional (1D) lattice of infinitely particles, each with mass M. The equilibrium distance is h. We can choose an arbitrary particle as the origin and number it 0. So the current position of particle n is given by

$$x_n = nh + u_n, \tag{51}$$

where u_n is the displacement of particle n. For the harmonic potential, the equation of motion is

$$m\ddot{u}_n = \frac{C}{h^2}(u_{n+1} + u_{n-1} - 2u_n). \tag{52}$$

Assume the following wave solution:

$$u_n = Ae^{i(\omega t - 2\pi knh)}, \tag{53}$$

where ω is the angular frequency, k is the wave number, and A is the amplitude. For the above expression to be the solution, the following condition has to be satisfied:

$$\omega^2 A = DA, \tag{54}$$

where

$$D = -\frac{C}{mh^2}(e^{-i2\pi kh} + e^{i2\pi kh} - 2), \tag{55}$$

Eq. (54) can be viewed as an 1D eigenvalue problem. The solutions of ω^2 are obtained as the eigenvalues of D, which is called the dynamic matrix. For real h, Eq. (54) reduces to

$$\omega^2 = \frac{4C}{mh^2}\sin^2 \pi kh. \tag{56}$$

This is the dispersion relationship between ω and k in the simple lattice.[15] One may find that only frequencies lower than a certain value ω_{crit} can be carried by the wave solution (53).

Now we study the dispersion in the PML region, where we have stretched atomic spacing h:

$$h \to h(1 - id_n). \tag{57}$$

Here $d_n := d(\mathbf{X}_n)$ is the damping function defined at each particle. The solution changes to

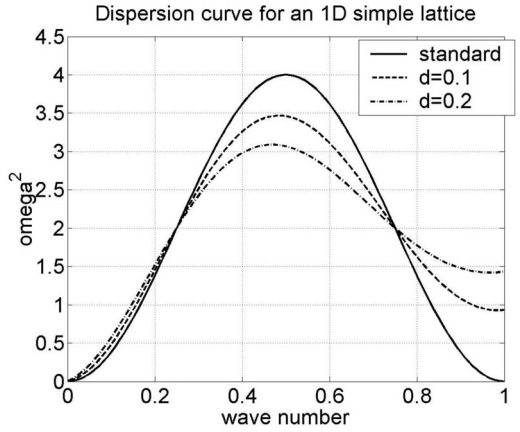

FIG. 1. The dispersion relation at the interface.

$$u_n = Ae^{i(\omega t - 2\pi knh)}e^{-2\pi knhd_n}. \tag{58}$$

Substituting the above expression into Eq. (52), we obtain

$$h^2\frac{m}{C}(1 - d_n^2 - 2id_n)\omega^2 = 2 - e^{-i2\pi kh}e^{-2\pi khd_{n+1}} - e^{i2\pi kh}e^{2\pi khd_{n-1}}. \tag{59}$$

This is the new dispersion relationship. It is much more complicated than the one in the original lattice (56). We are interested in the dispersion relation at the interface, which can give us an idea of which waves can travel into the PML region without distortion.

Assume that the interface is at the particle $n=0$. Furthermore, we let $d_0=0$, since the damping function is by our choice. Then we can re-write Eq. (59) as

$$\omega^2 A = \tilde{D}A, \tag{60}$$

where the stretched dynamic matrix $\tilde{D}$ has the following expression:

$$\tilde{D} = \frac{C}{mh^2}(2 - e^{-i2\pi kh}e^{-2\pi khd_1} - e^{i2\pi kh}e^{2\pi khd_{-1}}). \tag{61}$$

This is the dispersion relation at the interface. For ω^2 to have a real solution, we must have

$$d_{-1} = -d_1. \tag{62}$$

Again, the above equation is valid since we can choose d. With this choice, Eq. (61) reduces to

$$\omega^2 = \frac{2C}{mh^2}(1 - \cos 2\pi kh e^{-2\pi khd_1}). \tag{63}$$

This is the final dispersive relationship at the interface. We plot it in comparison with the dispersive relationship of the original lattice shown in Fig. 1.

Remark 3. (i) Based on Eq. (63), we can calculate the group velocity v_g:

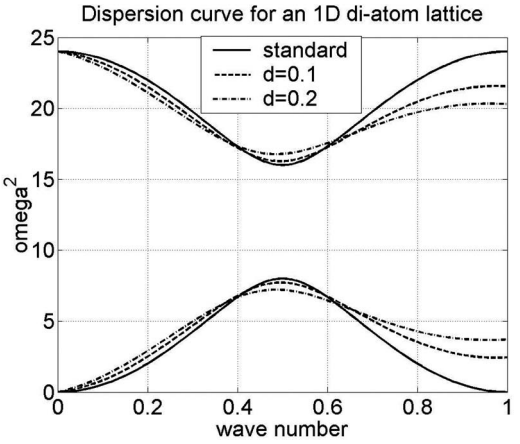

FIG. 2. The dispersion relation at the interface.

$$v_g = \frac{d\omega}{dk} = \frac{1}{\omega}\frac{C}{mh^2}(\sin 2\pi kh + 2\pi hd_1 \cos 2\pi kh)e^{-2\pi khd_1}. \tag{64}$$

So when $k \to \infty$, i.e., in the case of small wavelength, we will have a zero group velocity, which means that the PML zone looks like a continuum for small waves.

(ii) Assume $d_1 \leqslant 1$. Under long wavelength approximation, i.e., $2\pi kh \ll 1 \to 1 - \cos 2\pi kh \exp(-2\pi khd_1) \approx 0.5(2\pi kh)^2$. Based on Eq. (63),

$$\omega^2 = \left(\frac{C}{m}\right)(2\pi k)^2. \tag{65}$$

This again leads to the continuum limit. Therefore both cases imply that we have constructed a "transitional semidiscrete-semicontinuum layer" that can seamlessly couple a discrete region with a continuous region. This may be the meaning of the atomic distance stretching, or the meaning of the term "perfectly matched" for discrete systems.

(iii) In Figs. 2 and 3, at the right edge of the first half

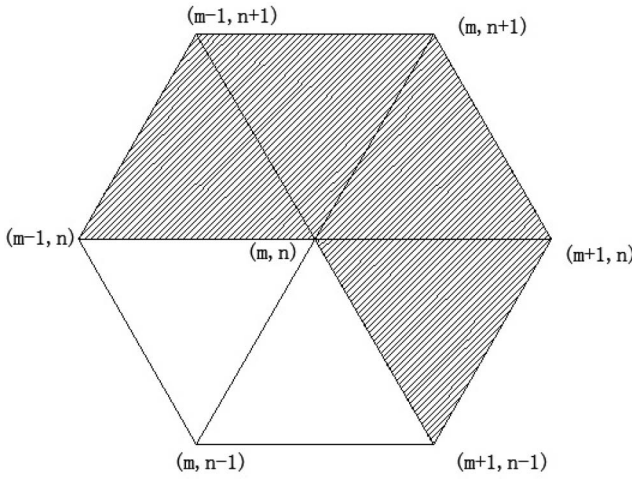

FIG. 3. Numbering in a hexagonal lattice. The shaded part is the PML region.

Brillouin zone, the wave frequency of a PML region is not zero. This is because the medium of a PML lattice is inhomogeneous, and thus the dispersive relations inside the Brillouin zone are no longer periodic.

It is clear that the original band structure of the dispersion relation has changed. More specifically, the bandwidth is *reduced*, which means waves with certain frequencies that can propagate along the regular (original) lattice cannot propagate into the PML zone directly. If they cannot propagate in the discrete PML zone, will they be reflected back? We will comment on this at the end of this section. For the moment, we first examine dispersive relations of PML zone for some other types of lattice.

Let us consider a 1D diatomic lattice. In particular we have

$$\text{particle with mass } m_1\text{: } X_{2n+1} = (2n+1)\frac{h}{2}, \tag{66}$$

$$\text{particle with mass } m_2\text{: } X_{2n} = nh. \tag{67}$$

Thus the period of the lattice is h, and the original distance between two neighboring particles is $0.5h$. We shall assume nearest-neighbor interaction. For a pair of particles $2n$ and $2n+1$, we have the following equations of motion:

$$m_0 \ddot{u}_{2n} = \frac{4C}{h^2}(u_{2n+1} + u_{2n-1} - 2u_{2n}), \tag{68}$$

$$m_1 \ddot{u}_{2n+1} = \frac{4C}{h^2}(u_{2n+2} + u_{2n} - 2u_{2n+1}). \tag{69}$$

The following wave solutions satisfy the above equations:

$$u_{2n} = A_0 e^{i(\omega t - 2n\pi kh)}, \tag{70}$$

$$u_{2n+1} = A_1 e^{i(\omega t - (2n+1)\pi kh)} \tag{71}$$

with the dispersive relation

$$\omega^2 \mathbf{A} = \mathbf{D}\mathbf{A}, \tag{72}$$

where $\mathbf{A} = [A_0, A_1]^T$ and dynamic matrix $\mathbf{D}$ has the following expression:

$$\mathbf{D} = \frac{8C}{m_0 m_1 h^2}\begin{bmatrix} m_1 & m_1 \cos \pi kh \\ m_0 \cos \pi kh & m_0 \end{bmatrix}. \tag{73}$$

The solution of the eigenvalue problem (72) is

$$\omega^2 = \frac{4C}{m_0 m_1 h^2}(m_0 + m_1 \pm \sqrt{m_0^2 + m_1^2 + 2m_0 m_1 \cos 2\pi kh}). \tag{74}$$

Now we consider the dispersion in PML region. In particular we are interested in the MD-PML interface to investigate the change of dispersion curve. So we shall consider particles $2n$, $2n+1$, $2n+2$, and $2n-1$, with the interface at particle $2n$. Similar to what we did to the simple lattice, we stretch h:

$$h \to h(1 - id_{2n}). \tag{75}$$

Then the assumed solutions will change to

$$\tilde{u}_{2n} = A_0 e^{i(\omega t - 2n\pi kh)} e^{-2n\pi khd_{2n}}, \tag{76}$$

$$\tilde{u}_{2n+1} = A_1 e^{i(\omega t - (2n+1)\pi kh)} e^{-(2n+1)\pi khd_{2n+1}}. \tag{77}$$

The new solutions satisfy the conditions

$$-\frac{m_0 h^2}{4C}(1 - d_{2n}^2 - 2id_{2n})A_0 e^{-2n\pi khd_{2n}}\omega^2 = A_1(e^{-i\pi kh-(2n+1)\pi khd_{2n+1}} + e^{i\pi kh-(2n-1)\pi khd_{2n-1}}) - 2A_0 e^{2n\pi khd_{2n}} \tag{78}$$

$$-\frac{m_1 h^2}{4C}(1 - d_{2n+1}^2 - 2id_{2n+1})A_1 \omega^2 e^{-(2n+1)\pi khd_{2n+1}} = A_0(e^{-i\pi kh-(2n+2)\pi khd_{2n+2}} + e^{i\pi kh-2n\pi khd_{2n}}) - 2A_1 e^{(2n+1)\pi khd_{2n+1}}. \tag{79}$$

Similar to the case of the 1D simple lattice, we let the damping coefficient

$$d_{2n} = 0 \tag{80}$$

at the interface. For the diatomic lattice, we further let

$$d_{2n+1} = 0. \tag{81}$$

This makes sense if we assume d being uniform in a *lattice cell* instead of being defined at a single atom.

Equations (78) and (79) then reduce to the following eigenvalue problem:

$$\omega^2 \mathbf{A} = \tilde{\mathbf{D}}\mathbf{A}, \tag{82}$$

where the $\tilde{D}$ is given by

$$\tilde{\mathbf{D}} = \frac{4C}{m_0 m_1 h^2}\begin{bmatrix} 2m_1 & \tilde{D}_{12} \\ \tilde{D}_{21} & 2m_0 \end{bmatrix} \tag{83}$$

and

$$\tilde{D}_{12} = (e^{-i\pi kh} + e^{i\pi kh} e^{-(2n-1)\pi khd_{2n-1}})m_1, \tag{84}$$

$$\tilde{D}_{21} = (e^{-i\pi kh} e^{-(2n+2)\pi khd_{2n+2}} + e^{i\pi kh})m_0. \tag{85}$$

The condition for the eigenvalue problem (82) to have real eigenvalues is

$$\mathrm{Im}[(e^{-i\pi kh} + e^{i\pi kh} e^{-(2n-1)\pi khd_{2n-1}}) \times (e^{i\pi kh} + e^{-i\pi kh} e^{-(2n+2)\pi khd_{2n+2}})] = 0. \tag{86}$$

That is equivalent to

$$d_{2n-1} = \frac{2n+2}{2n-1} d_{2n+2} \tag{87}$$

If the above condition is satisfied, we will have the following equation for ω^2:

$$\frac{m_0 m_1 h^4}{16C^2}\omega^4 - \frac{m_0 + m_1}{2C}\omega^2 - (2\cos 2\pi kh e^{-(2n+2)\pi khd_{2n+2}} + e^{-2(2n+2)\pi khd_{2n+2}} - 3) = 0 \tag{88}$$

which yields the solution

$$\omega^2 = \frac{4C}{m_0 m_1 h^2}\{m_0 + m_1 \pm [(m_0 + m_1)^2 - m_0 m_1 (3 - 2\cos 2\pi kh e^{-(2n+2)\pi k h d_{2n+2}} - e^{-2(2n+2)\pi k h d_{2n+2}})]^{1/2}\}. \tag{89}$$

The dispersion curves for standard diatomic lattice and the stretched lattice are shown in Fig. 2. The band gap is enlarged by PML, as expected.

The last type of lattice that we shall study is a two-dimensional (2D) hexagonal lattice. With only one equilibrium spacing h, the fundamental translation vectors are

$$\mathbf{k}_1 = h\mathbf{e}_1, \quad \mathbf{k}_2 = h\cos\frac{\pi}{3}\mathbf{e}_1 + h\sin\frac{\pi}{3}\mathbf{e}_2 = \frac{h}{2}\mathbf{e}_1 + \frac{\sqrt{3}h}{2}\mathbf{e}_2. \tag{90}$$

As we did in previous cases, we will use an integer pair (m,n) to identify a particle in the lattice. Suppose we already have a reference point $\mathbf{X}^{00}$, then

$$\mathbf{X}^{mn} = \mathbf{X}^{00} + m\mathbf{a}_1 + n\mathbf{a}_2. \tag{91}$$

In the harmonic case, the particles are connected by linear springs with axial stiffness C/h^2. We will assume small displacements. Then the equation of motion can be written as

$$mh^2\ddot{\mathbf{u}}^{mn} = \mathbf{C}_1(2\mathbf{u}^{mn} - \mathbf{u}^{m+1,n} - \mathbf{u}^{m-1,n}) + \mathbf{C}_2(2\mathbf{u}^{mn} - \mathbf{u}^{m,n+1} - \mathbf{u}^{m,n-1}) + \mathbf{C}_3(2\mathbf{u}^{mn} - \mathbf{u}^{m-1,n+1} - \mathbf{u}^{m+1,n-1}), \tag{92}$$

where $\mathbf{C}_i$ are stiffness matrices in three directions. They are

$$\mathbf{C}_1 = C\begin{bmatrix} 1 & 0 \\ 0 & 0 \end{bmatrix}, \tag{93}$$

$$\mathbf{C}_2 = C\begin{bmatrix} 1/4 & \sqrt{3}/4 \\ \sqrt{3}/4 & 3/4 \end{bmatrix}, \tag{94}$$

$$\mathbf{C}_3 = C\begin{bmatrix} 1/4 & -\sqrt{3}/4 \\ -\sqrt{3}/4 & 3/4 \end{bmatrix}. \tag{95}$$

Based on Eq. (45), we assume the solution to be

$$\mathbf{u}^{mn} = \mathbf{A}e^{i[\omega t - \mathbf{k}\cdot\mathbf{X}(m,n)]} \tag{96}$$

Substitute Eq. (96) into the equation of motion, we have

$$mh^2\omega^2\mathbf{A} = \mathbf{C}_1(2 - e^{-ik_1 h} - e^{ik_1 h})\mathbf{A} + \mathbf{C}_2(2 - e^{-ik_2 h} - e^{ik_2 h})\mathbf{A} + \mathbf{C}_3(2 - e^{i(k_1 - k_2)h} - e^{-i(k_1 - k_2)h})\mathbf{A}. \tag{97}$$

It can be further simplified as the following eigenvalue problem:

$$\omega^2\mathbf{A} = \mathbf{D}\mathbf{A}, \tag{98}$$

where

$$\mathbf{D} = \frac{2C}{mh^2}\begin{bmatrix} D_{11} & D_{12} \\ D_{21} & D_{22} \end{bmatrix}, \tag{99}$$

where

$$D_{11} = \frac{3}{2} - \cos k_1 h - \frac{1}{4}\cos k_2 h - \frac{1}{4}\cos(k_1 - k_2)h, \tag{100}$$

$$D_{12} = \frac{\sqrt{3}}{4}[\cos(k_1 - k_2)h - \cos k_2 h] \tag{101}$$

$$D_{21} = \frac{\sqrt{3}}{4}[\cos(k_1 - k_2)h - \cos k_2 h], \tag{102}$$

$$D_{22} = \frac{3}{2} - \frac{3}{4}\cos k_2 h - \frac{3}{4}\cos(k_1 - k_2)h. \tag{103}$$

The characteristic equation is

$$(mh^2\omega^2)^2 - 2Cmh^2(D_{11} + D_{22})\omega^2 + 4C^2(D_{11}D_{22} - D_{12}^2) = 0. \tag{104}$$

This is the dispersion equation for the regular hexagonal lattice. The solution has two branches:

$$\omega^2 = \frac{C}{mh^2}[D_{11} + D_{22} \pm \sqrt{(D_{11} - D_{22})^2 + 4D_{12}^2}]. \tag{105}$$

Now we stretch the lattice,

$$h \to h[1 - id(\mathbf{X})]. \tag{106}$$

We shall now look at the solution with h. Without losing generality, we let

$$\mathbf{X}^{00} = \mathbf{0}. \tag{107}$$

Assume particle (m,n) is at the interface, particles $(m,n-1)$, $(m-1,n)$, and $(m+1,n-1)$ are in the original lattice region, and particles $(m,n+1)$, $(m+1,n)$, and $(m-1,n+1)$ are in the PML zone as shown in Fig. 3. We then have

$$\mathbf{u}^{mn} = \mathbf{A}e^{i\omega t}e^{-i(mk_1 + nk_2)h}e^{-(mk_1 + nk_2)hd}. \tag{108}$$

Substituting the solution into Eq. (97) yields

$$\begin{aligned} mh^2[1 - id(\mathbf{X})]^2\omega^2 e^{-(mk_1 + nk_2)hd^{mn}}\mathbf{A} &= \mathbf{C}_1\mathbf{A}(2e^{-(mk_1 + nk_2)hd^{mn}} - e^{-ik_1 h}e^{-[(m+1)k_1 + nk_2]hd^{m+1,n}} \\ &- e^{ik_1 h}e^{-[(m-1)k_1 + nk_2]hd^{m-1,n}}) + \mathbf{C}_2\mathbf{A}(2e^{-(mk_1 + nk_2)hd^{m,n}} \\ &- e^{-ik_2 h}e^{-[mk_1 + (n+1)k_2]hd^{m,n+1}} - e^{ik_2 h}e^{-[mk_1 + (n-1)k_2]hd^{m,n-1}}) \\ &+ \mathbf{C}_3\mathbf{A}(2e^{-(mk_1 + nk_2)hd^{m,n}} \\ &- e^{i(k_1 - k_2)h}e^{-[(m+1)k_1 + (n-1)k_2]hd^{m+1,n-1}} \\ &- e^{-i(k_1 - k_2)h}e^{-[(m-1)k_1 + (n+1)k_2]hd^{m-1,n+1}}). \end{aligned} \tag{109}$$

Let

$$d^{mn} = 0 \tag{110}$$

and we further denote

$$\lambda^{m,n+1} = [(m+1)k_1 + nk_2]hd^{m+1,n} = [(m-1)k_1 + nk_2]hd^{m-1,n},$$

$$\lambda^{m,n+1} = [mk_1 + (n+1)k_2]hd^{m,n+1} = [mk_1 + (n-1)k_2]hd^{m,n-1},$$

$$\lambda^{m+1,n-1} = [(m+1)k_1 + (n-1)k_2]hd^{m+1,n-1} = [(m-1)k_1 + (n+1)k_2]hd^{m-1,n+1}.$$

Equation (109) can then be written as

$$mh^2\omega^2\mathbf{A} = 2[\mathbf{C}_3[1-\cos(k_1-k_2)he^{-\lambda^{m+1,n-1}}] + \mathbf{C}_2(1-\cos k_2 he^{-\lambda^{m,n+1}}) + \mathbf{C}_1(1-\cos k_1 he^{-\lambda^{m+1,n}})]\mathbf{A}. \quad (111)$$

Now the eigenvalue problem becomes

$$\omega^2\mathbf{A} = \tilde{\mathbf{D}}\mathbf{A} \quad (112)$$

with

$$\tilde{\mathbf{D}} = \frac{2C}{mh^2}\begin{bmatrix}\tilde{D}_{11} & \tilde{D}_{12}\\ \tilde{D}_{21} & \tilde{D}_{22}\end{bmatrix}, \quad (113)$$

where

$$\tilde{D}_{11} = \frac{3}{2} - \cos k_1 h \exp(-\lambda^{m+1,n}) - \frac{1}{4}\cos k_2 h \exp(-\lambda^{m,n+1}) - \frac{1}{4}\cos(k_1-k_2)h\exp(-\lambda^{m+1,n-1}), \quad (114)$$

$$\tilde{D}_{12} = \frac{\sqrt{3}}{4}[\cos(k_1-k_2)h\exp(-\lambda^{m+1,n-1}) - \cos k_2 h\exp(-\lambda^{m,n+1})], \quad (115)$$

$$\tilde{D}_{21} = \tilde{C}_{12}, \quad (116)$$

$$\tilde{D}_{22} = \frac{3}{2} - \frac{3}{4}\cos k_2 h\exp(-\lambda^{m,n+1}) - \frac{3}{4}\cos(k_1-k_2)h\exp(-\lambda^{m+1,n-1}). \quad (117)$$

The solutions then have a similar form to the one in original lattice:

$$\omega^2 = \frac{C}{mh^2}[\tilde{D}_{11} + \tilde{D}_{22} \pm \sqrt{(\tilde{D}_{11}-\tilde{D}_{22})^2 + 4\tilde{D}_{12}^2}]. \quad (118)$$

To explore the physical implication of the PMMS, we examine the dispersion relation pairs: Eq. (54) vs Eq. (60), Eq. (72) vs Eq. (82), and Eq. (99) vs Eq. (112). We observe that all three pairs of eigenvalue problems have the same structure, except that in the PML zone the dynamic stiffness matrices have spatial decaying terms. This suggests that the discrete absorbing PML zone is a direct consequence of the fact that propagation dispersive wave solutions are mapped into the similar dispersive wave solutions with exponentially decaying coefficients, which may be a general characterization of lattice PML.

The wave vector $\mathbf{k}$ can be defined in the reciprocal lattice:

$$\mathbf{k} = k_1\mathbf{b}_1 + k_2\mathbf{b}_2, \quad (119)$$

where $\mathbf{b}_i$ satisfy

$$\mathbf{b}_i \cdot \mathbf{a}_j = h\delta_{ij}. \quad (120)$$

It is ready to obtain that

$$\mathbf{b}_1 = \mathbf{e}_1 - \frac{1}{\sqrt{3}}\mathbf{e}_2, \quad \mathbf{b}_2 = \frac{2}{\sqrt{3}}\mathbf{e}_2. \quad (121)$$

Figure 4 shows the dispersion surfaces in the standard lattice and the stretched lattice. The two surfaces in each plot are on top of each other. The wave vector used is $\mathbf{k}=k_1\mathbf{b}_1+k_2\mathbf{b}_2$, with $k_1,k_2\in[0,2\pi]$. Note that although there are two branches in the hexagonal lattice, there is no band gap.

Remark 4. After examining the PML dispersive relations in several different lattices, we would like to make the following tentative remarks: (i) The band structure of the lattice changes in the PML zone; (ii) the range of admissible frequencies reduces in the PML region; and (iii) By choosing the suitable damping function, most of the admissible frequencies can be kept in the PML region.

As for those waves with frequencies inadmissible to the PML region, will they be completely reflected back? Or will they be transformed to other forms of waves? Currently we do not have the answer yet. We have performed numerical

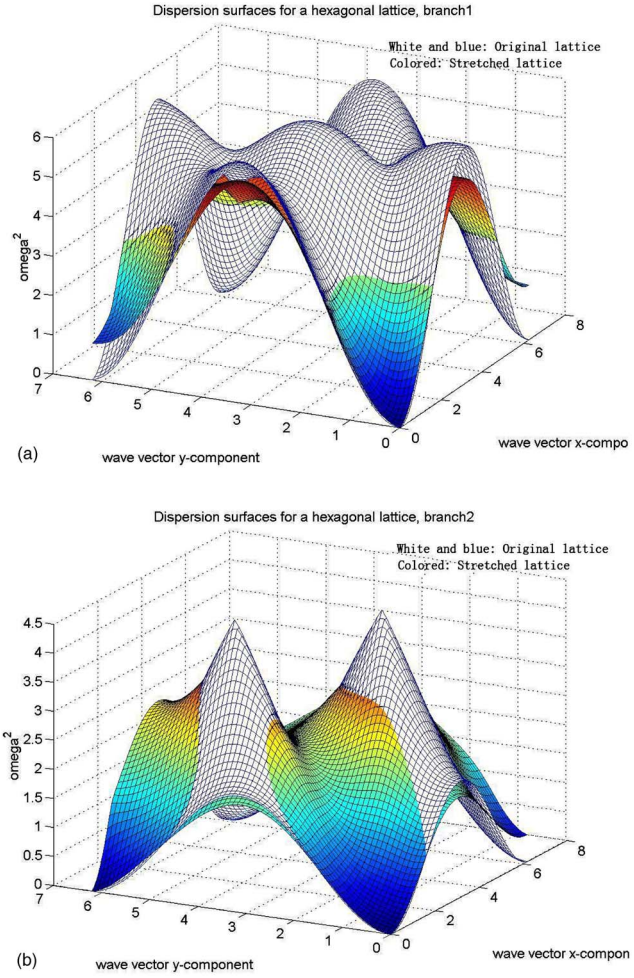

FIG. 4. (Color online) The dispersion surfaces of a hexagonal lattice: (a) branch 1, and (b) branch 2.

experiments, in which we let a harmonic wave with an inadmissible frequency passing into the PML region. We found that the wave is being suppressed, and there is not much reflection. So we are inclined to the second scenario that the wave may be converted into another wave. One possible explanation is that the wave is transformed into one with complex wave vectors. However, this hypothesis needs to be verified.

C. Reflection coefficient of a 1D simple lattice

Up to now, we have not discussed much about the damping function d, except on how to choose d near the interface. In this section, we shall examine how d will affect the reflection coefficient.

To make it simple, we use the 1D simple lattice as an example. We consider two 1D simple lattices $L1$ and $L2$. The former may be viewed as the regular lattice and the latter as the PML lattice. They are jointed at a point P, where the mass is imagined to be split into halves. The left half belongs to $L1$ and the right half belongs to $L2$.

We now examine the characteristic impedance. For a lattice extending from $(-\infty, nh]$, the impedance Z is defined as

$$f_{n,n+1} = -Z\dot{u}_n, \tag{122}$$

where $f_{n,n+1}$ is the force needed to be on particle n for a harmonic wave to travel without being reflected back. It is found that

$$Z = \frac{C}{h}\frac{\sin 2\pi kh}{\omega}. \tag{123}$$

In the case of a stretched lattice, the result is more complicated. It is more natural to think of the stretched lattice as extending from $[0, \infty)$. In this case, the impedance Z should be defined as

$$f_{-1,0} = Z\dot{u}_0. \tag{124}$$

We consider the equation of motion for the particle at interface, i.e., the 0th particle:

$$\frac{C}{h^2}(u_1 - u_0) + Z\dot{u}_0 = \frac{1}{2}mu_0. \tag{125}$$

Without loss of generality, we assume the general solution for u_n as

$$u_n = Ae^{i(\omega t - 2\pi knh)}e^{-2\pi knhd_n}. \tag{126}$$

Note that $d_0 = 0$. So,

$$u_0 = Ae^{i\omega t}, \tag{127}$$

$$u_1 = Ae^{i(\omega t - 2\pi ah)}e^{-2\pi khd_1}. \tag{128}$$

We then have the following equation of motion:

$$\frac{C}{h^2}(u_1 - u_0) + Z\dot{u}_0 = \frac{1}{2}mu_0. \tag{129}$$

Substitute u_0 and u_1 into the above equation, and we have the following result:

$$Z = Z_r + iZ_i, \tag{130}$$

$$Z_r = \frac{C}{h^2}\frac{\sin 2\pi khe^{-2\pi khd_1}}{\omega}, \tag{131}$$

$$Z_i = \frac{C}{h^2\omega}\left(\cos 2\pi khe^{-2\pi khd_1} - 1 + \frac{1}{2}m\omega^2\right). \tag{132}$$

Note that when $d_1 = 0$, we recover the result for the regular lattice.

The energy flow through the lattice is then defined by

$$Q = \frac{1}{2}\,\mathrm{Re}(Z)|\dot{u}_n|^2. \tag{133}$$

Now consider a wave traveling to the interface. We denote the incident wave I, transmitted wave T, and reflected wave R. Assume the initial position for point P is

$$X_p = ph, \tag{134}$$

where p is an integer. Then the displacements are assumed to be

$$u_I = A_Ie^{i(\omega t - 2\pi kph)}, \tag{135}$$

$$u_T = A_Te^{i(\omega t - 2\pi kph)}e^{-2\pi kphd_p}, \tag{136}$$

$$u_R = A_Re^{i(\omega t + 2\pi kph)}. \tag{137}$$

But we should have $d_p = 0$, since P is the beginning of the PML zone. So we write the equations again:

$$u_I = A_Ie^{i(\omega t - 2\pi kph)}, \tag{138}$$

$$u_T = A_Te^{i(\omega t - 2\pi kph)}, \tag{139}$$

$$u_R = A_Re^{i(\omega t + 2\pi kph)}. \tag{140}$$

The conservation of energy requires

$$Q_I = Q_T + Q_R. \tag{141}$$

The condition for two halves of the particle P to move together is

$$A_T = A_I + A_R \tag{142}$$

and the reflection coefficient R is defined as

$$R = \frac{A_R}{A_I}. \tag{143}$$

It is not difficult to obtain the following relation:

$$R = \frac{Z_1 - Z_2}{Z_1 + Z_2}. \tag{144}$$

From the previous discussion, we have

$$Z_1 = \frac{C}{h}\frac{\sin 2\pi kh}{\omega}, \tag{145}$$

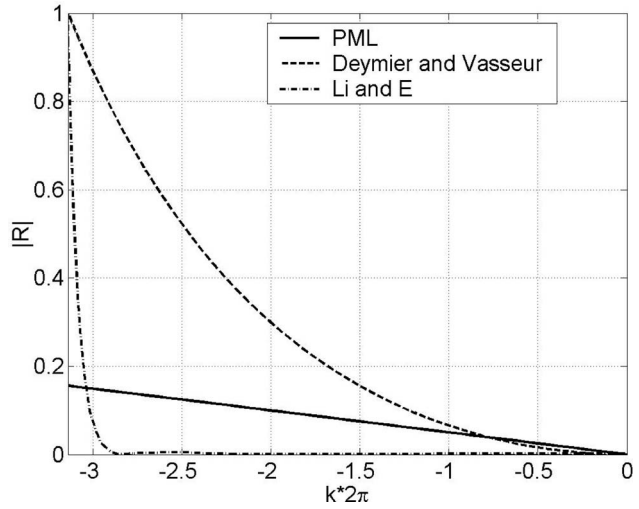

FIG. 5. The reflection coefficient vs reduced angular frequency.

$$Z_2 = \frac{C}{h^2}\frac{\sin 2\pi k h e^{-2\pi k h d_1}}{\omega}. \tag{146}$$

Then

$$R = \frac{1 - e^{-2\pi k h d_1}}{1 + e^{-2\pi k h d_1}}. \tag{147}$$

It is of interest to study R as a function of k. By doing so, one can show how well waves with a specific wave number are transmitted into the PML zone. Reflection coefficients for three different concurrent methods are plotted versus reduced angular frequencies in Fig. 5. For PMMS, the damping coefficient d is chosen to be 0.1 in this example. We observe that the reflection coefficient is almost zero at the low frequency (long wavelength) limit, and it increases as the frequency increases. It stays lower than 0.2 at the end of the first Brillouin zone. For comparison purpose, we also showed in Fig. 5 the result obtained from the concurrent method with a variational boundary condition (VBC) developed by Li and E,[3] and the result obtained from the method with an atomic-elastic boundary developed by Deymier and Vasseur.[12] One may find that the PML has an obvious advantage at the high-frequency end as both other BCs' reflection coefficient approach 1. For the lower frequencies, the PML still does a good job. Its reflection coefficient is lower than that of the atomic-elastic boundary and higher than that of the VBC. Moreover, compared to the VBC, the PML has a lower computational cost, since the VBC is nonlocal in time.

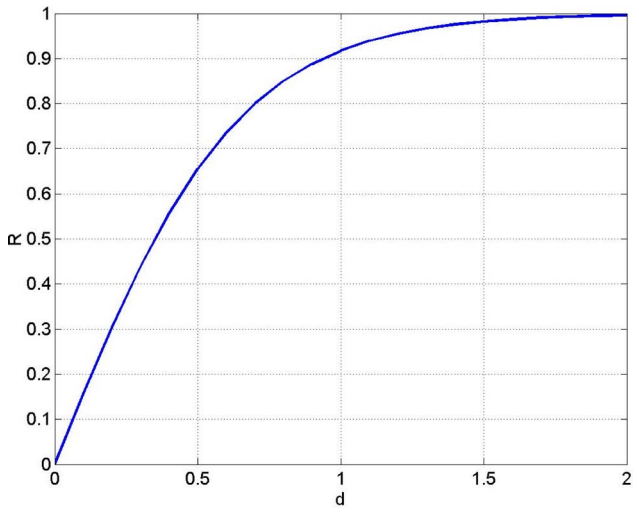

FIG. 6. (Color online) The reflection coefficient vs d_n.

We also want to study the effect of the damping function d. A plot of R against d_1 is shown in Fig. 6. We observe that R approaches 1 as d increases. So although a larger d_1 will make the PML solution decay faster [see Eq. (126)], it will also give a bigger reflection. Therefore we have to judiciously choose damping function d close to the interface in order to achieve optimal results. It is worth mentioning that by recalling Eq. (63),

$$\frac{1}{2}m\omega^2 = \frac{C}{h^2}(1 - \cos 2\pi k h e^{-2\pi k h d_1}), \tag{148}$$

and comparing it with Eq. (132) we obtain $Z_i = 0$. This agrees with the result of standard lattices, which makes sense.

V. APPLICATIONS

The implementation of the revised PMMS is almost the same as the one described in the original paper.[9] For the case with harmonic approximation, they are exactly the same. As expected, the computational results are only slightly affected. So in this section, we shall present only one example from the original paper and devote the remaining part to multiple dimensional problems.

We re-calculated the 1D wave propagation example in the original paper. A 1D lattice is considered. The interatomic potential is chosen to be the Lennard-Jones potential:

$$\phi(r) = 4\epsilon\left[\left(\frac{\sigma}{r}\right)^{12} - \left(\frac{\sigma}{r}\right)^{6}\right] \tag{149}$$

with $\sigma = \epsilon = 1$. We prescribe an initial displacement:

$$u_0(x) = \frac{A}{A - u_c}(Ae^{-(x/\sigma)^2} - u_c)\left[1 + b\cos\left(\frac{2\pi x}{H}\right)\right], \tag{150}$$

where

$$u_c = Ae^{-(r_c/\sigma)^2}. \tag{151}$$

The parameters are chosen as $A = 0.15$, $\sigma = 5.0$, $H = \sigma/4$, $r_c = 5\sigma$, and $b = 0.1$. The equilibrium bond distance is $h = 2^{1/6}$. We simulate this problem with 181 atoms and 60 FE elements. The coarse scale time step is 0.1 and the fine scale time step is 0.002.

Figure 7 shows the displacement at $t = 20$. Results calculated by both PMMS and MD (600 atoms) are shown. We can see only the low-frequency part of the wave passing into the coarse scale region. And there are very small reflections.

The second example is the 2D version of the previous 1D example. The initial condition is axis-symmetric and the ra-

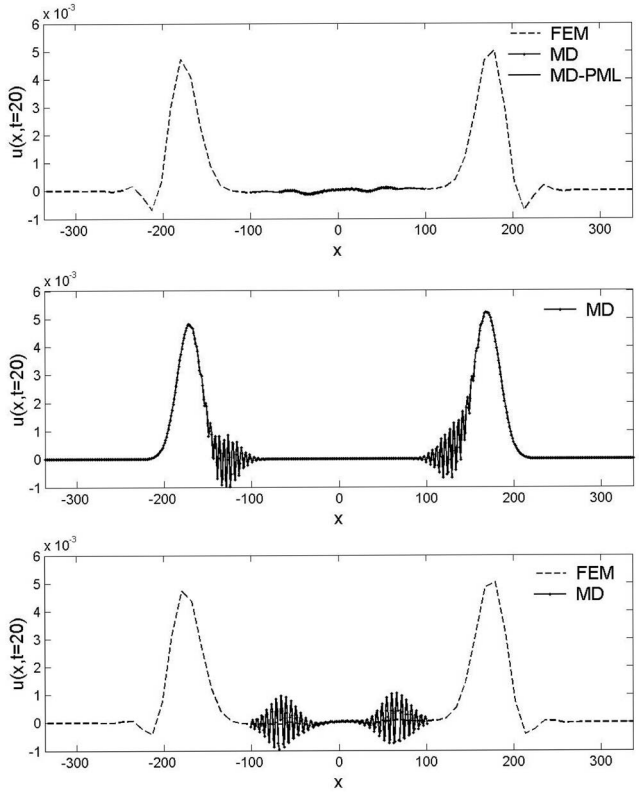

FIG. 7. The 1D wave problem: displacement at $t=20$: (a) PMMS solution, (b) the exact MD solution, and (c) a multiscale solution without PML.

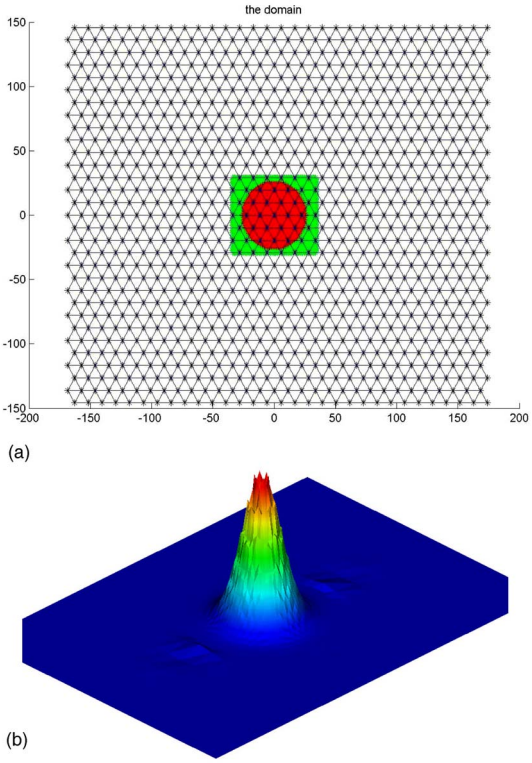

FIG. 8. (Color online) The 2D wave problem: (a) the problem domain, and (b) the problem's initial condition.

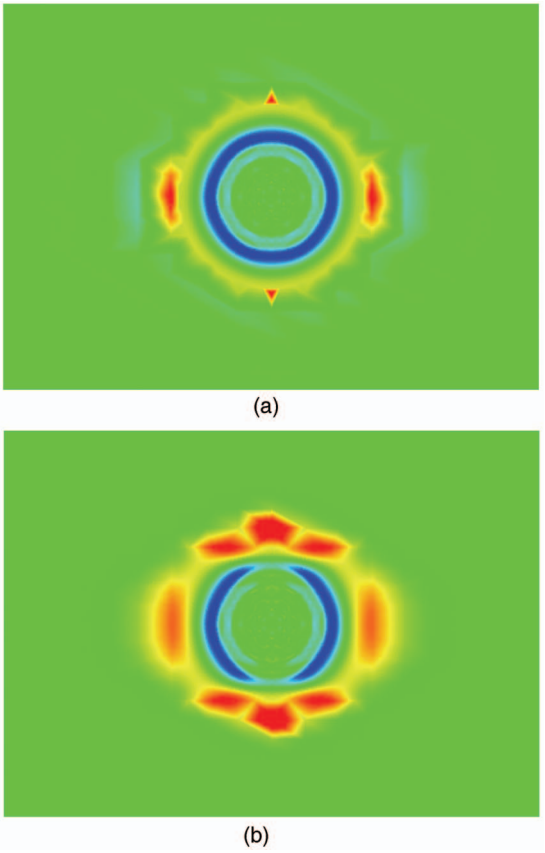

FIG. 9. (Color) The displacement profile of the 2D wave problem: (a) with PML, and (b) without PML.

dial component has the same expression as Eq. (150). The lattice is of hexagonal type. The dimension of the domain is $300h$ in width and $150\sqrt{3}h$ in height. The fine scale region is chosen to be $50h$ in width and the PML region has five layers. We simulate the problem with 61×61 atoms and 1800 FE elements. Figure 8 shows the domain, the MD region, the PML region, and the initial condition.

Figure 9 shows the displacement profile at the 210th coarse scale time step. Here we compare the PMMS results with the one without the PML region. We can see clearly from the figure that reflection occurs at the interface without the PML region. On the other hand, if we put a PML zone in, the reflection will be significantly reduced.

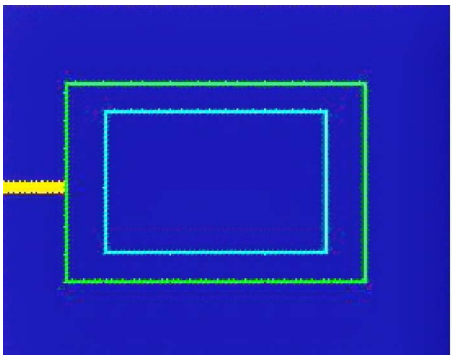

FIG. 10. (Color online) The domain of the screw dislocation simulation.

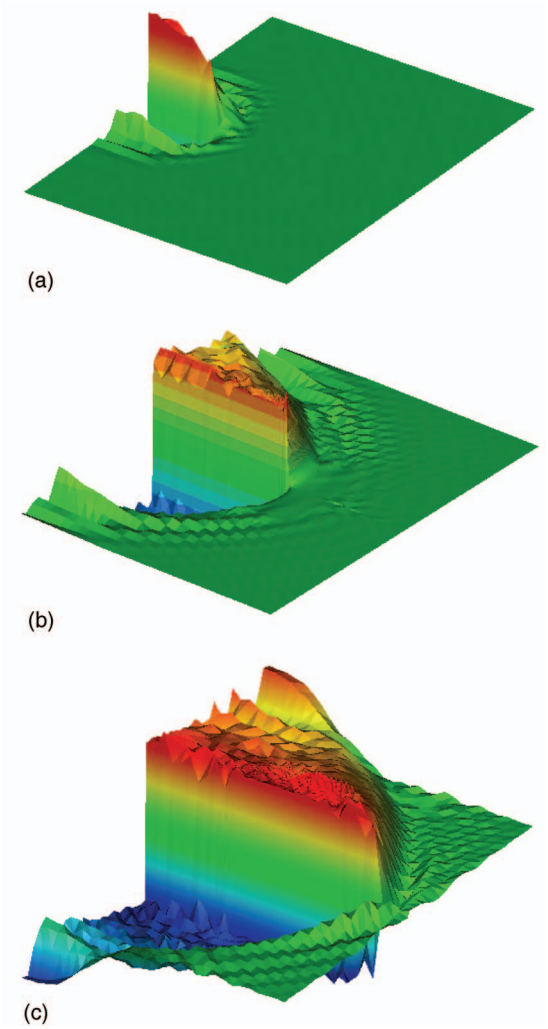

FIG. 11. (Color) The displacement profile of the screw dislocation problem (with PMMS): (a) dislocation starts from the coarse region, (b) dislocation enters the fine region, and (c) dislocation enters the coarse region again.

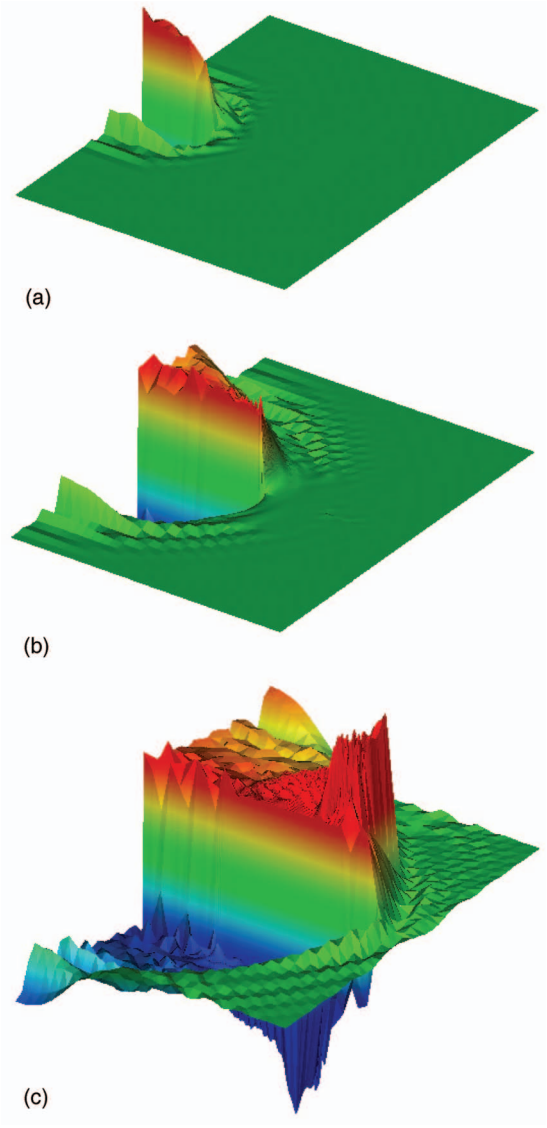

FIG. 12. (Color) The displacement profile of the screw dislocation problem (without PMMS): (a) dislocation starts from the coarse region, (b) dislocation enters the fine region, and (c) dislocation enters the coarse region again.

In the last example, we are applying the proposed PMMS method to simulate a screw dislocation passing through regions with different scales, i.e., spatial resolution. First the screw dislocation enters a fine scale region modeled by MD from a coarse scale region modeled by quasicontinuum FE, then it travels through the fine scale region, and it re-enters the coarse scale region.

The 2D molecular-dynamics model used is based on Refs. 19 and 20. The domain is two dimensional but only the out-of-plane displacement is considered. The underlying lattice structure is cubic. The neighboring atoms are assumed to connected by springs with z-direction stiffness. The dislocation is initiated in the coarse scale region. It propagates into the fine scale region and then re-enters the coarse scale region. The MD equation of motion in the fine scale region can be written as[19]

$$m_a \ddot{w}^{m,n} = A(w^{m+1,n} + w^{m-1,n}) + B(w^{m,n+1} + w^{m,n-1}) - 2(A+B)w^{m+n} - Bb(\delta_{m,k+1/2}\delta_{n,1/2} + \delta_{m,k+1/2}\delta_{n,-1/2}), \quad (152)$$

where A and B are force constants between an atom and his x-direction neighbors and y-direction neighbors, respectively. b is the length of Burger's vector, and $w(m,n)$ is the out-of-plane direction displacement of atom (m,n), which has an in-plane position of

$$\mathbf{X}^{(m,n)} = mh\mathbf{e}_1 + nh\mathbf{e}_2, \quad m,n = \ldots, -\frac{3}{2}, -\frac{1}{2}, \frac{1}{2}, \frac{3}{2}, \ldots. \quad (153)$$

Here h is the equilibrium distance. The dislocation is assumed to be in the $n=0$ plane.

The dimension of the whole domain is 150×200. The fine scale region has a dimension of 70×70 and the PML region has ten layers of atoms. The positions of the three

different regions are illustrated in Fig. 10. The initial equilibrium distances are 1. We simulated the problem with 2556 atoms and 650 FE elements.

When a dislocation propagating, opposite cohesive forces due to dislocation gliding are applied to the pair of atoms located next to the dislocation plane $\left(n=\pm\frac{1}{2}\right)$. A so-called "quarter jump" rule [21] is adopted as the dislocation propagation criterion, i.e., when the displacement of the atom ahead of the dislocation reaches to $b/4$, we consider that the dislocation has passed this atom already and apply the dislocation force to the next pair of atoms lying on the propagation direction. To simulate a screw dislocation moving in a coarse scale region modeled by the quasicontinuum method,[22] we exploit a procedure called "cohesive quasicontinuum method," which is the combination of the cohesive FEM technique[23,24] and the quasicontinuum method. A detailed discussion of that method will be reported in a separated paper.[25]

Figures 11(a)–11(c) show the propagating dislocation at different stages by using PMMS. For comparison, Figs. 12(a)–12(c) show the simulation results without the PML region. It is found that although the dislocation can pass through the fine scale region successfully, it causes significant reflection when re-entering the coarse scale region.

VI. CONCLUSIONS

In this paper, we present the latest developments of PMMS. In particular, we have found that (i) the lattice PML can be constructed by stretching the lattice constant in the Fourier domain; (ii) the physical meaning of such lattice constant stretching operation is equivalent to replacing the original lattice stiffness with certain complex lattice stiffness; (iii) the form of the dispersive relation in the PML zone is the same of that in the original lattice, expect that the stretched dynamic stiffness matrix contains spatial decaying terms, and consequently, the lattice PML becomes an absorbing boundary layer; (iv) the PML zone may serve as a low-pass filter, because the bandwidth of admissible frequencies is usually reduced in the PML zone; (v) the reflection coefficient at the interface can be controlled by choosing the damping function, and (vi) we have demonstrated that by using the PMMS technique we easily pass a defect (dislocation in the example) from a scale to another scale.

The fact of bandwidth change in the PML zone leaves a door open for other possible approaches to construct perfectly matched layers. For example, instead of using complex coordinate stretching, we can try to construct a different *physical* lattice in the PML region with gradual impedance change, or, using some techniques suggested in Ref. 18, construct a special microstructure for PML zone. This may also suppress the wave solution in the PML zone without causing significant phonon reflection. This topic will be a future research subject. Finally, we would like to mention that a finite temperature (thermalized) version of PMMS is currently being implemented, which will be reported in a separate paper.

ACKNOWLEDGMENTS

This work was supported by a grant from NSF (Grant No. CMS-0239130), which is greatly appreciated.

*Electronic address: li@ce.berkeley.edu

[1] W. E and Z. Huang, Phys. Rev. Lett. **87**, 135501 (2001).
[2] W. E, B. Engquist, and Z. Huang, Phys. Rev. B **67**, 092101 (2003).
[3] X. Li and W. E, Commun. Comput. Phys. **1**, 136 (2006).
[4] G. J. Wagner and W. K. Liu, J. Comput. Phys. **190**, 249 (2003).
[5] G. J. Wagner, E. G. Karpov, and W. K. Liu, Comput. Methods Appl. Mech. Eng. **193**, 1579 (2004).
[6] H. S. Park, E. G. Karpov, P. A. Klein, and W. K. Liu, Philos. Mag. **85**, 79 (2005).
[7] R. E. Rudd and J. Q. Broughton, Phys. Rev. B **58**, R5893 (1998).
[8] R. E. Rudd and J. Q. Broughton, Phys. Rev. B **72**, 144104 (2005).
[9] A. To and S. Li, Phys. Rev. B **72**, 035414 (2005).
[10] J. Berenger, J. Comput. Phys. **114**, 185 (1994).
[11] F. Collino and C. Tsogka, Geophysics **66**, 294 (2001).
[12] P. A. Deymier and J. O. Vasseur, Phys. Rev. B **66**, 134106 (2002).
[13] W. K. Liu, E. G. Karpov, S. Zhang, and H. S. Park, Comput. Methods Appl. Mech. Eng. **193**, 1529 (2004).
[14] W. C. Chew and W. H. Weedon, Microwave Opt. Technol. Lett. **7**, 599 (1994).
[15] L. Brillouin, *Wave Propagation in Periodic Structures*, 2nd ed. (Dover, New York, 1946).
[16] C. Kittel, *Introduction to Solid State Physics*, 8th ed. (John Wiley & Sons, Hoboken, NJ, 2005).
[17] M. M. Sigalas and E. N. Economou, J. Sound Vib. **158**, 377 (1992).
[18] P. G. Martinsson and A. B. Mouchan, Q. J. Mech. Appl. Math. **56**, 45 (2003).
[19] K. C. King and T. Mura, J. Phys. Chem. Solids **52**, 1019 (1993).
[20] T. Mura, *Micromechanics of Defects in Solids* (Kluwer, Dordrecht, 1987).
[21] A. A. Maradudin, J. Phys. Chem. Solids **9**, 1 (1958).
[22] E. B. Tadmor, M. Ortize, and R. Philips, Philos. Mag. A **73**, 1529 (1996).
[23] X.-P. Xu and A. Needleman, J. Mech. Phys. Solids **42**, 1397 (1994).
[24] M. Ortiz and A. Pandolfi, Int. J. Numer. Methods Eng. **44**, 1267 (1999).
[25] X. Liu and S. Li (unpublished).